Dovepress

ORIGINAL RESEARCH

Mitochondria-Rich Microvesicles Alleviate CNI ED by Transferring Mitochondria and Suppressing Local Ferroptosis

Zhenkang Liang*, Zehong Chen*, Chaowei Zhang, Cui Chen, Wende Yang, Yuxuan Zhang, Hongbo Wei

Department of Gastrointestinal Surgery, The Third Affiliated Hospital of Sun Yat-Sen University, Guangzhou, 510630, People's Republic of China

*These authors contributed equally to this work

Correspondence: Hongbo Wei, Department of Gastrointestinal Surgery, The Third Affiliated Hospital of Sun Yat-sen University, Tianhe Road 600, Guangzhou, 510630, People's Republic of China, Tel +86-020-85253000, Email weihb@mail.sysu.edu.cn

Purpose: Erectile dysfunction (ED) frequently arises as a complication of pelvic surgeries, including rectal and prostate surgery, and has no definitive cure. This study explored whether mitochondria-rich microvesicles (MVs) can be used to treat ED stemming from cavernous nerve injury (CNI) and investigated its potential mechanisms.

Methods: We isolated MVs and mitochondria (MT) from PC12. The apoptosis rate, mitochondrial membrane potential (MMP), reactive oxygen species (ROS), mitochondrial derived reactive oxygen species (mtROS), iron content, malondialdehyde (MDA) content and endogenous antioxidant system activity of corpus cavernosum smooth muscle cells (CCSMCs) cultured with MVs and MT were detected in vitro. In vivo, twenty-four male Sprague Dawley rats were randomly divided into four groups: sham operation group and CNI group were injected with PBS, MVs and MT respectively. After fourteen days of treatment, the erectile function was measured and penile tissues were collected for histological analysis. Subsequently, inhibition of mitochondria in MV was performed to explore the mechanism of the rescue experiment.

Results: The CCSMCs, PC12-MVs and PC12-MT were successfully isolated and identified. After MVs culture, apoptosis rate, ROS, mtROS, iron content and MDA content of CCSMCs were significantly decreased, while MMP and the activities of endogenous antioxidant system were increased. MVs transplantation can significantly restore erectile function and smooth muscle content in CNIED rats. The rescue experiment suggested that MVs exerted the above therapeutic effect by transferring mitochondria within it.

Conclusion: MVs transplantation significantly improve erectile function in CNI ED rats. MVs may play a role in anti-OS and anti-ferroptosis at the transplant site through efficient transfer of mitochondria, providing a potential treatment vehicle for CNI ED.

Keywords: cavernous nerve injury, erectile dysfunction, microvesicles, oxidative stress, ferroptosis

Introduction

Erectile dysfunction (ED) is characterized by an inability to attain and maintain an erection suitable for satisfactory sexual intercourse.[1] One specific type of ED is cavernous nerve injury (CNI)-related ED, which typically occurs after pelvic surgeries such as radical resection of rectal cancer.[2,3] Although surgical methods based on protecting nerve function have been proposed, patients still suffer from CNI ED, which is a common symptom after surgery.[4,5] Currently, oral phosphodiesterase type 5 inhibitor (PED5i) drugs, vacuum erection devices, drug injections, and other treatment methods are available for CNI ED, but none of them achieve the desired effect.[2,6,7] Therefore, there is an urgent need to develop novel therapeutic approaches.

Extracellular vesicles (EVs) have attracted widespread attention as novel agents for treating diseases.[8–10] These vesicles can be categorized into exosomes (Exos) and microvesicles (MVs) based on their size and can be effectively isolated using methods such as filtration and gradient centrifugation.[11,12] Some studies have found that MVs may contain

intact mitochondria or mitochondrial components, which is one of the mechanisms through which they exert therapeutic effects.[13,14] Currently, researchers are using MVs to repair damaged cardiomyocytes and restore energy supply to cardiomyocytes.[15,16] However, the therapeutic effects of these MVs on CNI ED remain unexplored.

PC12 is a rat adrenal pheochromocytoma cell line that can differentiate into sympathetic ganglion neurons under the induction of nerve growth factor (NGF) and is widely used in neuroscience research.[17] Nerve cells are among the most energy-intensive cell types in humans owing to their crucial role in the transmission of electrical signals, which results in a large number of mitochondria that provide ATP.[18] PC12-derived exosomes and mitochondria (MT) have shown promising therapeutic effects against various diseases.[19,20] In addition, after CNI, the ability of the corpus cavernosum (CC) to respond to signals from various neural pathways was significantly weakened, and neurotrophic loss occurred. Being in this state for an extended period inevitably leads to ED.[21] This may allow MVs derived from nerve cells to play a role in treatment. However, to the best of our knowledge, the use of PC12 cell-derived MVs as a therapeutic modality for CNI ED has rarely been studied.

Oxidative stress (OS) is a key part of the pathogenesis of many diseases, including atherosclerosis, chronic blocking lung disease, and spinal cord injury.[22] This process involves the disruption of the balance between oxidants and antioxidants, leading to the accumulation of excessive reactive oxygen species (ROS) or other free radicals. Consequently, this imbalance triggers apoptosis, tissue damage, and other detrimental outcomes.[23] A study has demonstrated that the reduction of OS can restore erectile function in rats with diabetic ED.[24] Additionally, OS and apoptosis have been observed within the cavernosum of CNI ED rats.[25] However, the question of whether MVs can decrease the level of OS and apoptosis in CNI ED remains unanswered.

Ferroptosis represents a distinct mode of OS, characterized by a core mechanism that entails lipid peroxidation.[26] This process ultimately results in the destruction of cell membranes and the induction of cell death. Ferroptosis has been linked to numerous diseases, including degenerative disorders and ischemia-reperfusion injury.[26,27] Recently, ferroptosis was also observed in the cavernosal smooth muscle in rat models of diabetic ED and CNI ED.[28–30] However, whether MVs can improve the efficacy of CNI ED by inhibiting ferroptosis remains unclear.

Currently, there is no literature on the effects of MVs on OS, apoptosis or ferroptosis. We isolated MT and MVs from PC12 cells and they were implanted into CNI ED rat models to compare their therapeutic effects on CNI ED and their possible therapeutic mechanisms were further explored.

Materials and Methods
Cells Cultures and Characterization

The PC12 were purchased from the ATCC, whereas the corpus cavernosum smooth muscle cells (CCSMCs) were derived from the cell bank in our laboratory which were extracted primary smooth muscle cells from the cavernosum of rats.[31] All experiments in this search have allowed by the Ethics Committee of Experimental Animals at South China Agricultural University (2024D018). All liquids used to culture cells are filtered with 0.22 μm filter to remove MVs that may be present in them. CCSMCs were cultured in high-glucose DMEM (Gibco, USA), containing 10% MV-free fetal bovine serum (FBS) (Gibco, USA) and 1% penicillin-streptomycin (Gibco, USA), and cultured in a 5% CO_2 incubator at 37 °C. The CCSMCs were identified via immunofluorescence staining (See 2.12 for details). CCSMCs were cultured in serum-free high-glucose DMEM containing varying concentrations of H_2O_2 (Aladdin, China) ranging from 0 to 1000 μM, for 4 h to establish in vitro models of OS in CCSMCs. Similarly, the cells were cultured in serum-free high-glucose DMEM containing varying concentrations of RSL3 (MCE, USA), ranging from 0 to 2 μM, for 24 h to establish in vitro models of ferroptosis in CCSMCs.

To induce well differentiation of PC12, cells were cultured in high-glucose DMEM containing 50 μM nerve growth factor (NGF) (PeproTech, USA), supplemented with 10% MVs-free FBS and 1% penicillin-streptomycin at 37 °C and 5% CO_2.[17] PC12 cells were identified using immunofluorescence (See 2.12 for details).

Cell Proliferation Assays

Cell viability was assessed using the CCK8 assay (Biosharp, China). CCSMCs were seeded with 3000 cells per well in 96-well culture plates and incubated overnight, the medium was changed to conduct the corresponding models as

described before, and 10% CCK8 solution was added after the processing time. After 1 h, the absorbance at 450 nm was measured using a microplate reader (BioTek Eon, USA).

Isolation and Identification of PC12-MVs and MT

PC12 cells were used for mitochondrial isolation following the instructions provided with a mitochondrial isolation kit (Beyotime, China). MVs were isolated through multistep centrifugation according to described methods described.[32] When the PC12 cells reached 80% confluence, the media were removed and centrifuged to collect the MVs. Dead cells were eliminated using centrifugation at 800 ×g for 10 min and 2500 ×g for 15 min. The supernatant was centrifuged at 10,000 ×g for 30 min, resuspended in PBS, and used for subsequent experiments. All the above centrifugation steps were performed at 4 °C.

Transmission electron microscopy (TEM) was used to examine the ultrastructure and morphological characteristics of the isolated PC12-MT and MVs. The mitochondrial protein markers COX IV (1:1000; Proteintech) and VDAC1 (1:1000; Proteintech) were identified and quantified by Western blotting. The size distribution of the MVs was determined using ZetaView PMX120 (ParticleMetrix, Germany).

PC12-MVs and MT Uptake in vitro and in vivo

In vitro, CCSMCs were incubated with labeled MT (100 μg/mL) or MVs (50 μg/mL) at 37 °C for 24 h. The CCSMCs were then immunostained with phalloidin (Servicebio, China), and the nuclei were stained with DAPI (Biosharp, China). In vivo, after CNI, the labeled MT (400 μg/mL) or MVs (200 μg/mL) were injected into the CC instantly, and the CC were collected 24 h after injection to prepare frozen sections. Smooth muscle was immunostained with α-smooth muscle actin (SMA) antibody (1:200; Cell Signaling Technology) and the nuclei were stained with DAPI. The resulting fluorescence signals were evaluated using a fluorescence microscope (Nikon, Japan).

Detection of Cellular ATP Content

To determine the optimal therapeutic dose of MVs, we used increasing doses of MVs to pretreat CCSMCs for 24 h before injury, as described previously. Subsequently, an ATP detection kit (Beyotime, China) was used to determine the ATP content of the cells in each group.

Apoptosis Assays

Cell apoptosis was assessed using the Annexin V-FITC/PI Apoptosis Detection Kit (KeyGEN Biotech, China) according to the manufacturer's instructions. Apoptosis was detected using flow cytometry (BD FACSCanto, USA).

Detection of MMP, ROS, and mtROS

The specific assay kits were employed to determine the intracellular levels of mitochondrial membrane potential (MMP), ROS, and mitochondria derived active oxygen species (mtROS). (MMP Assay kit with TMRE, ROS Assay kit, Beyotime; MitoSOX™ Red mitochondrial superoxide indicator, Invitrogen).

Iron, MDA, GSSG, and GSH Content Detection

The levels of intracellular malondialdehyde (MDA) and oxidized glutathione (GSSG) represent oxidative capacity, whereas glutathione (GSH) levels represent antioxidant capacity. The MDA, GSSG, and GSH contents in CCSMCs and CC were detected using an MDA assay kit (Beyotime, China) and a GSH assay kit (Beyotime, China) according to the manufacturer's protocols. The iron content in CCSMCs was assessed using an iron assay kit (Solarbio, China), whereas the iron content in CC was assessed using an iron assay kit (Nanjing Jiancheng, China). The absorbance was measured using a microplate reader.

Inhibition of Mitochondrial Function Within MVs

To verify whether mitochondria within MVs play a major therapeutic role, we inhibited mitochondrial function within MVs, as described previously.[15] After MVs were exposed to 10 mm 1-methyl-4-phenylpyrindinium (MPP+, Bidepharm,

China) for 90 min, they were centrifuged at 10,000 ×g for 30 min at 4 °C, then resuspended in PBS and used for subsequent experiments.

Animals and Experimental Design

A total of 48 male SD rats (8-week-old) were purchased from Sun Yat-sen University and housed in the Animal Experimental Center of South China Agricultural University. Animal experiments were approved by the Ethics Committee of Experimental Animals at South China Agricultural University (2024D018), and follow the animal experiment standard GB/T 42011–2022.

Rats were anesthetized by sevoflurane inhalation. The median incision of the abdomen was approximately 3 cm, and the CN, located in the lateral part of the dorsal lobe of the prostate, was crushed for 2 min to establish a CNI ED model in SD rats.[31]

A total of 24 male SD rats were randomly divided into four groups (n = 6 per group). The Sham group underwent laparotomy only, whereas the remaining three groups received BCNI followed by intracavernous injection (IC) of PBS (100 μL; PBS group), MVs (1×10^9 MVs; MV group), or MT (100 μg MT; MT group).

Another 24 male SD rats were randomly distributed into four groups (n = 6 per group). The Sham group underwent laparotomy alone, whereas the remaining three groups underwent BCNI and were subsequently injected with PBS (100 μL; PBS group), MPP+ MVs (1×10^8 MPP+ MVs; MPP+ group), or MVs (1×10^8 MVs; MV group).

Erectile Function Assessment

Two weeks after surgery, the intracavernous pressure (ICP) and mean arterial pressure (MAP) of the animals were recorded to assess erectile function. Following anesthesia, the unilateral carotid artery was isolated and a heparinized 24-G cannula was inserted to record the MAP. The CC was dissected, and a heparinized 25-G butterfly needle was inserted into the root of the penis for ICP measurement. Subsequently, the rat CN was accessed via a ventral median incision. The proximal segment was chosen as the stimulation site, and the parameters were set at 1.5 mA, 20 hz, and 50s to elicit penile erection. All data were recorded using the BL-420S Biological Function System (Chengdu Taimeng Technology Ltd., China). Following the experiments, the penile tissue was collected for further histological evaluation and Western Blot analysis.

Fluorescence and Masson's Trichrome Staining

To label MVs and MT, PC12 cells were incubated with 200 nM Mitotracker Red CMXRos (MTRC) (Invitrogen, USA) before MT and MVs were isolated.

In accordance with the manufacturer's instructions, the levels of OS and mitochondrial superoxide in the CC were measured using ROS and MitoSOX assays. DAPI was used to stain cell nuclei.

To perform immunohistochemical staining, sections of penile tissue were prepared at a thickness of 4 μm. Penile sections were incubated with primary antibodies against α-SMA (1:200; Cell Signaling Technology). CCSMCs were incubated with primary antibodies against α-smooth muscle actin (SMA) antibody (1:200; Cell Signaling Technology), Calponin antibody (1:200; Santa Cruz Biotechnology), GPX4 (1:200; affinity) and ACSL4 (1:200; affinity). PC12 were incubated with primary antibodies against microtubule-associated protein 2 (MAP2) antibody (1:200; Proteintech). Goat anti-rabbit IgG (CY3 conjugated) (1:500; Affinity), FITC-labeled goat anti-rabbit IgG (1:500; Biosharp), and FITC-conjugated goat anti-mouse IgG (1:1000; Proteintech) were used as secondary antibodies. Nuclei were stained with DAPI.

Masson's trichrome staining revealed that the smooth muscle appeared red, and the collagen fibers appeared blue. This allowed the smooth-muscle-to-collagen ratio in the CC to be determined and used to assess the degree of fibrosis. ImageJ 1.46 (National Institutes of Health, Bethesda, MD, USA) was used for the quantitative analysis of the images.

Western Blotting

In accordance with the manufacturer's instructions, proteins were extracted using a protein extraction reagent containing RIPA buffer (Beyotime, China) and protease inhibitors (Beyotime, China). Protein concentration was detected using a BCA Kit (Bestbio, China), and 30 μg of proteins were added to each lane to electrophoresis. After electrophoresis,

proteins were transferred onto polyvinylidene fluoride membranes and blocked with tris-buffered saline-Tween (5% skim milk powder). The membranes were then incubated overnight at 4 °C with the following primary antibodies: α-SMA (1:1000, Cell Signaling Technology), GPX4 (1:1000, Affinity), ACSL4(1:1000, Affinity), GAPDH (1:10,000, ABclonal).

Statistical Analysis

The data were expressed as the mean ± standard error of mean. All data collected in this study were analyzed using GraphPad Prism version 9.4 (GraphPad, USA). Differences among groups were compared using one-way analysis of variance (ANOVA), followed by Tukey's post-hoc analysis. Statistical significance was set at $P < 0.05$.

Result

Characterization of CCSMCs, PC12, MVs, and MT

CCSMCs exhibited characteristic spindle and fibroblast-like morphologies, and these cells were positively identified through the expression of α-SMA and calponin (Figure 1A and B). Poorly differentiated PC12 cells exhibited a polygonal shape and tended to aggregate (Figure 1C). After 72 h induction by 50 μM NGF, poorly differentiated PC12 differentiated into well differentiated form, with fusiform appearance, synaptic elongation, and increased expression of neural marker MAP2 (Figure 1C). Furthermore, before isolating MVs and MT, the quality and quantity of mitochondria in PC12 cells were assessed. Upon staining with MitoTracker Red CMXRos (MTRC), PC12 displayed intense red fluorescence (Figure 1D), which was indicative of substantial mitochondrial content within PC12.

MVs were isolated from the culture medium of PC12 cells, and MT were extracted directly from the cells. To determine the size distribution of the MVs, nanoparticle tracking analysis was performed, which revealed that the MVs primarily ranged from 150–300 nm (Figure 1E). TEM indicated that the morphology of the MVs and MT was intact, and that there was a membrane structure surrounding the MVs (Figure 1F). The expression of COX IV and VDAC 1 (mitochondrial marker proteins) was also observed in MVs and MT (Figure 1G). These results demonstrated that the isolated MVs and MT were complete and purified.

MVs Transplantation Alleviated Oxidative Stress CCSMCs

To determine whether MVs and MT were transferred to CCSMCs, they were labeled with MTRC and incorporated into the culture medium. After 2 h, cells were stained with phalloidin. The presence of MVs and MT in CCSMCs was confirmed by the observation of red-fluorescent mitochondria embedded within the green cytoskeleton (Figure 2A). CCSMCs were the main component of the penis and apoptosis of CCSMCs appeared after CNI; therefore, CCSMCs were used for modeling.[33,34] Many studies have shown that apoptosis and OS are found in the cavernosum after CNI, and the proteins involved in OS are significantly changed,[25,35] so we treated CCSMCs with different concentrations of H_2O_2 to simulate the local oxidative stress damage after CNI. Compared with the blank group (0μM), after treatment with 200, 400, 600, 800, and 1000 μM for 4 h, the cell morphology was changed, and the cell viability was significantly reduced when exposed to 600 μM (Figure 2B and C). Hence, 600 μM H_2O_2 was selected for subsequent analyses. To determine the optimal therapeutic dose of MVs, we used three doses: low (1×10^7), medium (5×10^7), and high (1×10^8) and found that the amount of ATP recovered was positively correlated with the therapeutic dose (Figure 2D). Next, we confirmed that MT (10 μg protein) obtained the same amounts of mitochondrial proteins (VDAC1 and COX IV) in approximately 1×10^8 MVs (Figure 2E-G).

The transfer efficiency of the MVs and MT was determined by measuring the MMP of the CCSMCs. Flow cytometry showed that the MMP was higher in the MV group than in the MT group (Figure 3A and B). The rate of apoptosis was evaluated in each group. The apoptosis rate of the MV and MT groups decreased when exposed to H_2O_2, and the decrease was more notable in the MV group (Figure 3C and D). When exposed to H_2O_2, fluorescence microscopy showed an increase in both cellular ROS and mtROS (Figure 3E-H). Compared to the control group, intracellular ROS levels decreased significantly after pretreatment with MVs (Figure 3E and G). Analogously, pretreatment with MVs exhibited the capability to diminish the generation of mtROS in CCSMCs (Figure 3F and H). These results suggest that
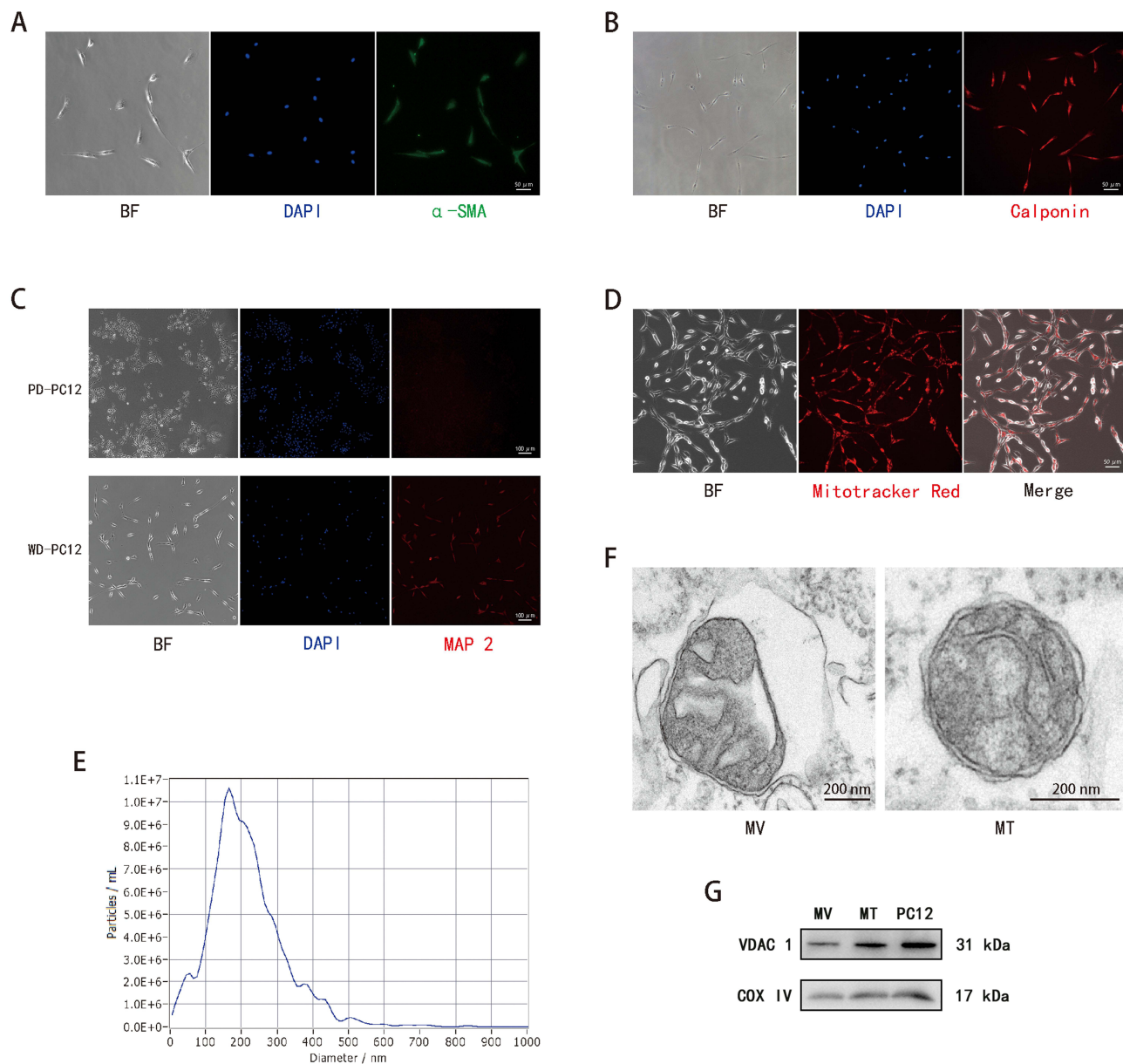
Figure 1 (**A**, **B**) Identification of CCSMCs using bright field and immunofluorescence with anti-α-SMA and anti-calponin antibody, scale bar, 50 μm. (**C**) Identification of poorly and well differentiated PC12 using bright field and immunofluorescence with anti-MAP 2, scale bar, 100 μm. (**D**) PC12 were stained with a mitochondrial specific indicator, Mitotracker Red CMXRos, scale bar, 50 μm. (**E**) Particle size distribution of the MVs measured using nanoparticle tracking analysis. (**F**) Transmission electron microscopy of MVs and MT, scale bar, 200nm. (**G**) Western blotting for MVs, MT and PC12 against mitochondria markers (VDAC1 and COX IV).

both MVs and MT could restore cellular energy supply and reduce intracellular OS, thereby reducing apoptosis in CCSMCs.

MV Transplantation Repressed Ferroptosis Through GPX4/ACSL4 Pathway in CCSMCs

Based on the assessment of cell morphology and viability, a concentration of 0.5 μM RSL3 was determined as the optimal concentration for our experiments (Figure 4A and B). After stimulating RSL3 for 24 h, ferroptosis was successfully induced in CCSMCs. MV and MT inhibited the increase in iron content caused by ferroptosis, down-regulated MDA and GSSG levels, and increased GSH levels (Figure 4C–F). However, the MV group exhibited a more robust resistance to ferroptosis than the MT group.
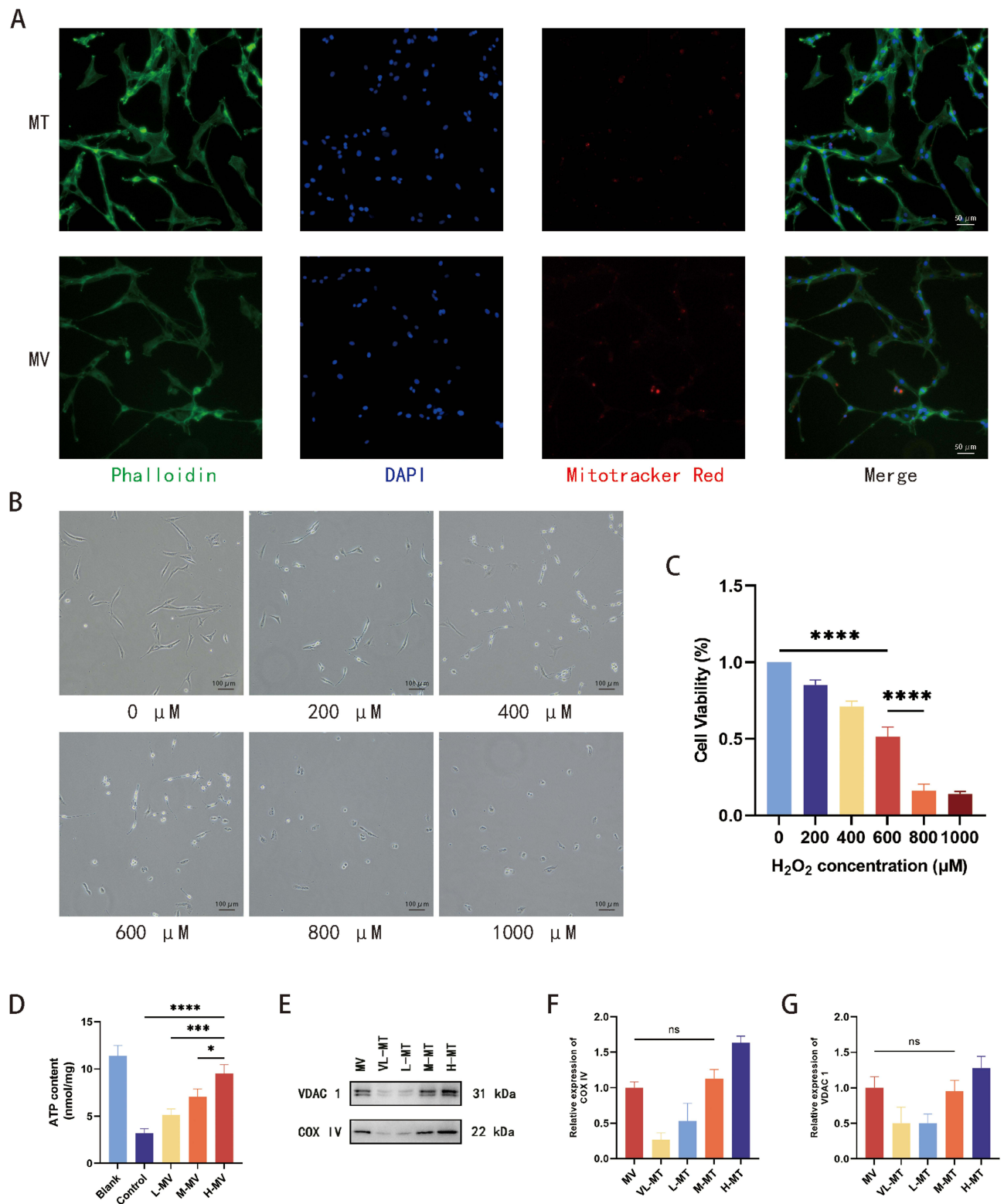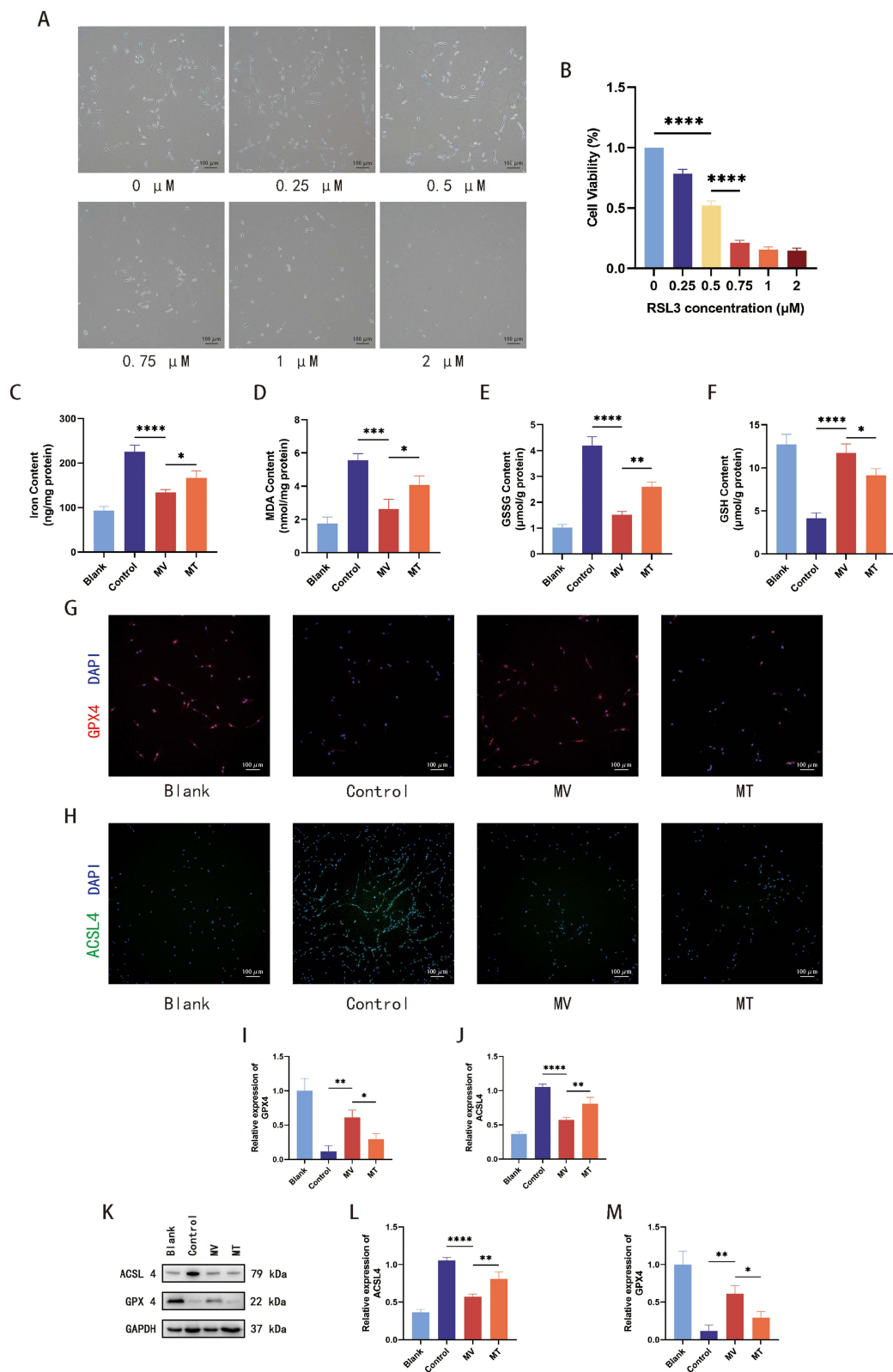
Figure 2 (**A**) PC12 derived MVs and MT uptake in vitro, scale bar, 50 μm. (**B, C**) The cell morphology and viability of CCSMCs were changed after treatment with different concentrations of H_2O_2 for 4 h, scale bar, 100 μm. (**D**) The adenosine triphosphate levels in CCSMCs were detected after different amounts of MV pretreatment. (**E-G**) Western blotting and quantitative analysis of MVs (1.0×108) and MT (2, 4, 10, 15 μg protein) for VDAC1 and COX IV. MT (10 μg protein) harbored the same amounts of mitochondrial proteins as those of 1.0×108 MVs (n=3). *P<0.05, ***P<0.001, ****P<0.0001.
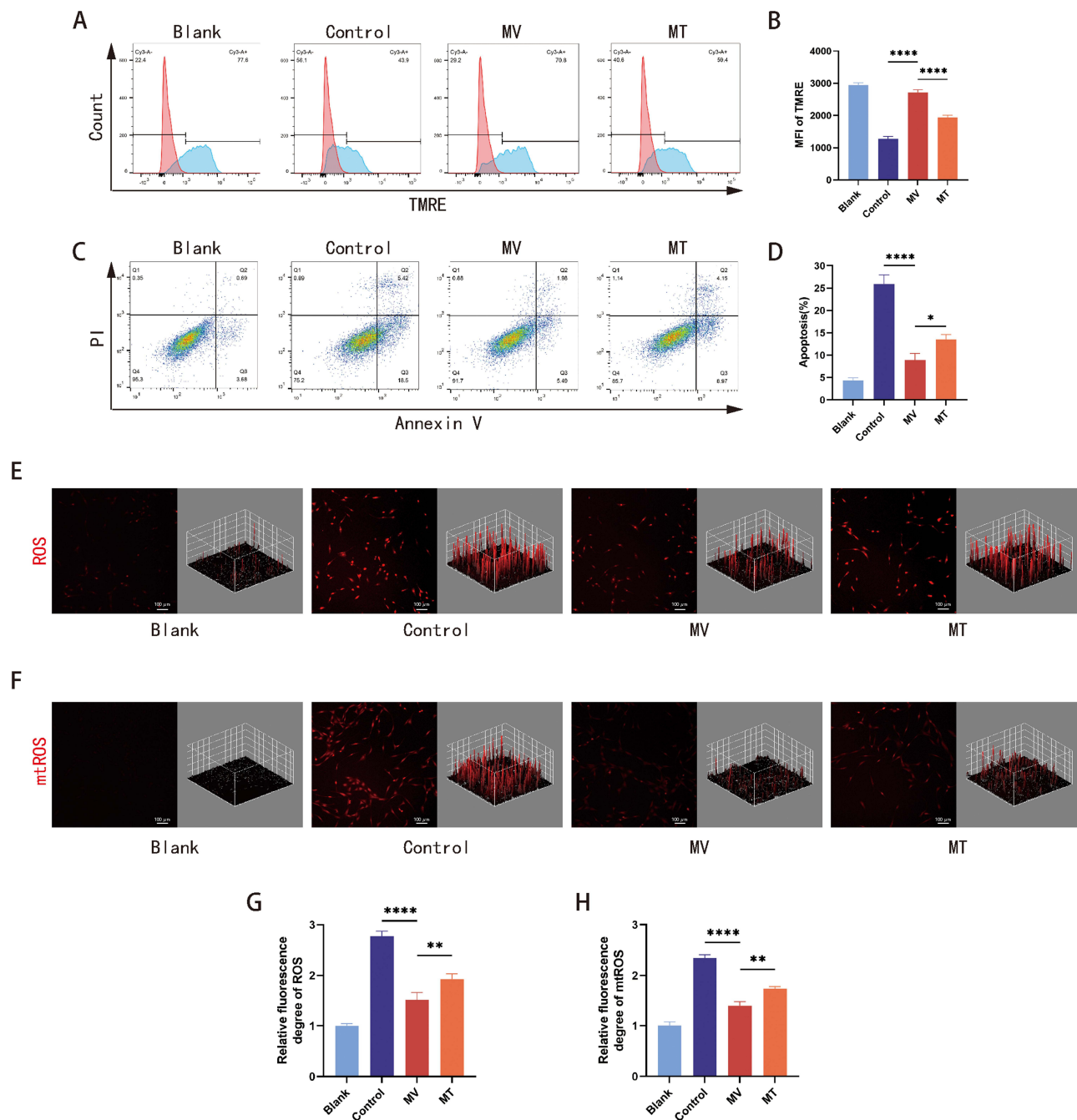
Figure 3 (**A** and **B**) The mitochondrial membrane potential of each group was analyzed using TMRE staining and flow cytometry (n=3). (**C** and **D**) Apoptosis in each group under H_2O_2 stimulation was analyzed using Annexin V-FITC/PI staining and flow cytometry (n=3). (**E** and **G**) Intracellular ROS levels in each group were determined using DHE-ROS and fluorescence microscope, scale bar, 100 μm (n=3). (**F** and **H**) Mitochondrial superoxide levels of each group were determined using MitoSOX and fluorescence microscope (n=3). Blank, CCSMCs without any treatment. Control, CCSMCs treated with H_2O_2 treatment. MV, CCSMCs pretreated with MVs before treating with H_2O_2 treatment. MT, CCSMCs pretreated with MT before treating with H_2O_2 treatment. *P<0.05, **P<0.01, ****P<0.0001. MFI: mean fluorescence intensity.

We explored whether MVs resist ferroptosis in CCSMCs via the GPX4/ACSL4 pathway. Fluorescence analysis of GPX4 and ACSL4 indicated that both the MV and MT groups had an inhibitory effect on RSL3-induced ferroptosis in CCSMCs. However, the MV group exhibited significantly stronger inhibition of the ferroptosis pathway than the MT group (Figure 4G–J). Similarly, both the MV and MT groups exhibited enhanced GPX4 expression and reduced expression ACSL4 but MVs had a superior effect (Figure 4K–M). In summary, MV transplantation represses ferroptosis through the GPX4/ACSL4 pathway in CCSMCs, and its suppressive effects are superior to those of MT.

Figure 4 (**A** and **B**) The cell morphology and cell viability of CCSMCs were changed after 24 h treatment with different concentrations of RSL3, scale bar, 100 μm. (**C-F**) The contents of iron content, MDA, GSSG, and GSH in CCSMCs were measured (n=3). (**G-J**) Representative fluorescence images and relative fluorescence degree of GPX4 and ACSL4 in CCSMCs of each group, scale bar, 100 μm (n=3). (**K-M**) Representative images of Western blot assays and relative protein expression levels of GPX4 and ACSL4 in CCSMCs of each group (n=3). Blank, CCSMCs without any treatment. Control, CCSMCs treated with RSL3 treatment. MV, CCSMCs pretreated with MVs before treating with RSL3 treatment. MT, CCSMCs pretreated with MT before treating with RSL3 treatment. *P<0.05, **P<0.01, ***P<0.001, ****P<0.0001.

MV Transplantation Ameliorated ED in CNI ED Rats

As shown in the diagram, we established the CNI ED rat model and evaluated the therapeutic effects of MVs and MT (Figure 5A). Twenty-four hours after injection, MVs- or MT-labeled red color was observed in the smooth muscle, which stained green (Figure 5B). The erectile function of the rats was evaluated by determining the ratio of ICP to MAP induced by electrical stimulation of the CN. The ratios of maximal ICP (ICP max) to MAP and total ICP (area under the curve) to MAP decreased in the PBS group (Figure 5C, D, G and H) but increased in the MV and MT groups after injection (Figure 5C-H). These findings demonstrate that both MVs and MT have the potential to alleviate ED in rats with CNI ED. Notably, MVs exhibited superior therapeutic efficacy compared with MT.

PC12-MV Transplantation Renewed Cavernosum Smooth Muscle Content

Atrophy of the CN is a key factor in ED. After measuring the erectile function, the CC was collected for subsequent analysis. Immunofluorescent staining of SMA in the penis served as an indicator of smooth muscle content. Notably, the PBS group displayed significantly reduced SMA expression compared to the sham group (Figure 6A and C). In contrast, both the MV and MT groups displayed higher SMA expression levels than the PBS group, with the MV group demonstrating superior improvement (Figure 6A and C). Masson's trichrome staining revealed a lower smooth muscle to collagen ratio in the PBS group than in the sham group (Figure 6B and D). Conversely, both the MV and MT groups exhibited a notable increase in the ratio of smooth muscle to collagen; however, the MV group demonstrated a greater increase in this ratio (Figure 6B and D). Similarly, the results of Western blotting were consistent with those of the SMA fluorescence analysis and Masson's trichrome staining. Both MVs and MT restored SMA expression, and MVs showed a better recovery effect (Figure 6E–F).

## MV Transplantation Therapy Attenuated Oxidative Stress and Ferroptosis in the CC

To investigate the extent of OS in CC following CNI, the fluorescence intensities of both cellular and mitochondrial superoxide levels were examined. Analysis of cellular and mitochondrial superoxide fluorescence revealed that the PBS group exhibited significantly elevated levels of ROS and mtROS in the CC compared to the sham group (Figure 7A–D). However, following transplantation with MVs or MT, a notable decrease was observed in the expression of these OS markers. MVs demonstrated superior improvement compared to MT (Figure 7A–D). These findings suggest that MVs effectively inhibit OS in the CC.

We observed that the levels of iron, MDA, and GSSG in the PBS group were significantly higher than those in the sham group (Figure 7E–G). Conversely, the GSH content in the PBS group was significantly lower than that in the sham group (Figure 7H). Transplantation of MVs and MT resulted in a reduction in iron, MDA, and GSSG content, while concomitantly increasing GSH content in the CC (Figure 7E–H). Meanwhile, the MV group showed further inhibition of iron, MDA, and GSSG content, and a significant improvement in GSH content compared to the MT group (Figure 7E–H).

Subsequently, the expression of the key molecules involved in the ferroptosis regulatory pathway was investigated. As shown by the Western blotting results, compared to the sham group, the expression of the negative regulator GPX4 was downregulated, whereas that of the positive regulator ACSL4 was upregulated in the PBS group (Figure 7I–K). Although both the MV and MT groups reversed these changes, the reversal effect in the MV group was significantly greater than that in the MT group (Figure 7I–K). Based on the above results, we conclude that MV transplantation enhances erectile function by attenuating OS and ferroptosis.

Therapeutic Effect Disappeared After Inhibiting the Mitochondrial Function Inside MVs

We performed rescue experiments to investigate whether MVs played a therapeutic role. To this end, mitochondria were transformed within MVs and MPP+ was used to inhibit mitochondrial function. The results showed that the ability of MVs to restore MMP decreased after MPP+ pretreatment (Figure 8A and B). Compared to the MV group, the apoptosis rate of the MPP+ group increased significantly and was close to that of the control group (Figure 8C and D). Furthermore, after treatment with MPP+, the levels of cellular and mitochondrial superoxide fluorescence intensity were enhanced, whereas these results were decreased in the MV group (Figure 8E–H). Subsequently, we pretreated
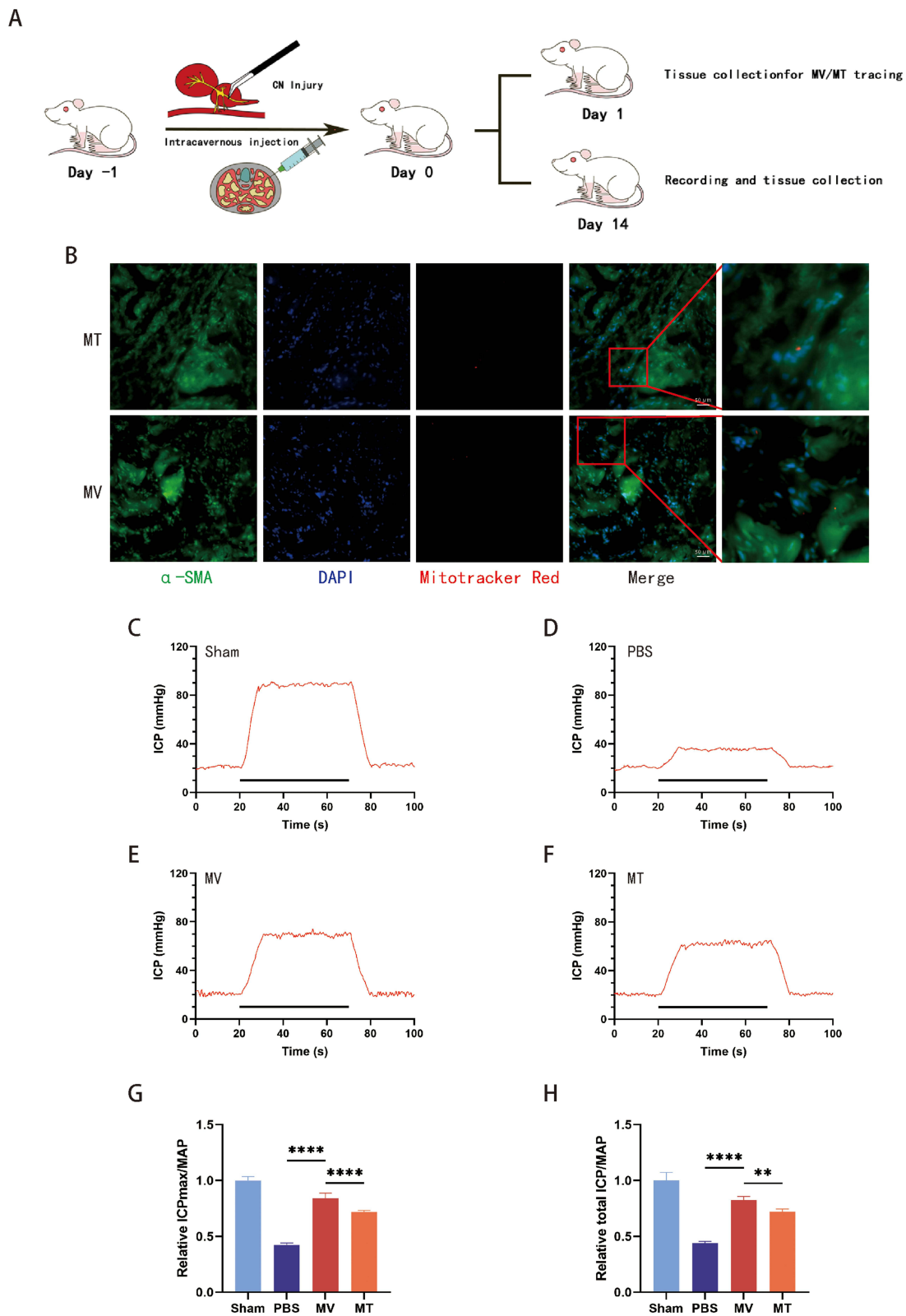
Figure 5 (**A**) Diagram of study design and experimental flowchart. (**B**) PC12 derived MVs and MT uptake in vivo, scale bar, 50 μm. (**C-F**) ICP responses to electrostimulation in the Sham, PBS, MV, and MT groups. (**G** and **H**) Relative ICPmax to MAP ratio, and total ICP to MAP ratio responses to electrostimulation in four groups (n=6). PBS, group injected with PBS. MV, group injected with MVs. MT, group injected with MT. **P<0.01, ****P<0.0001.
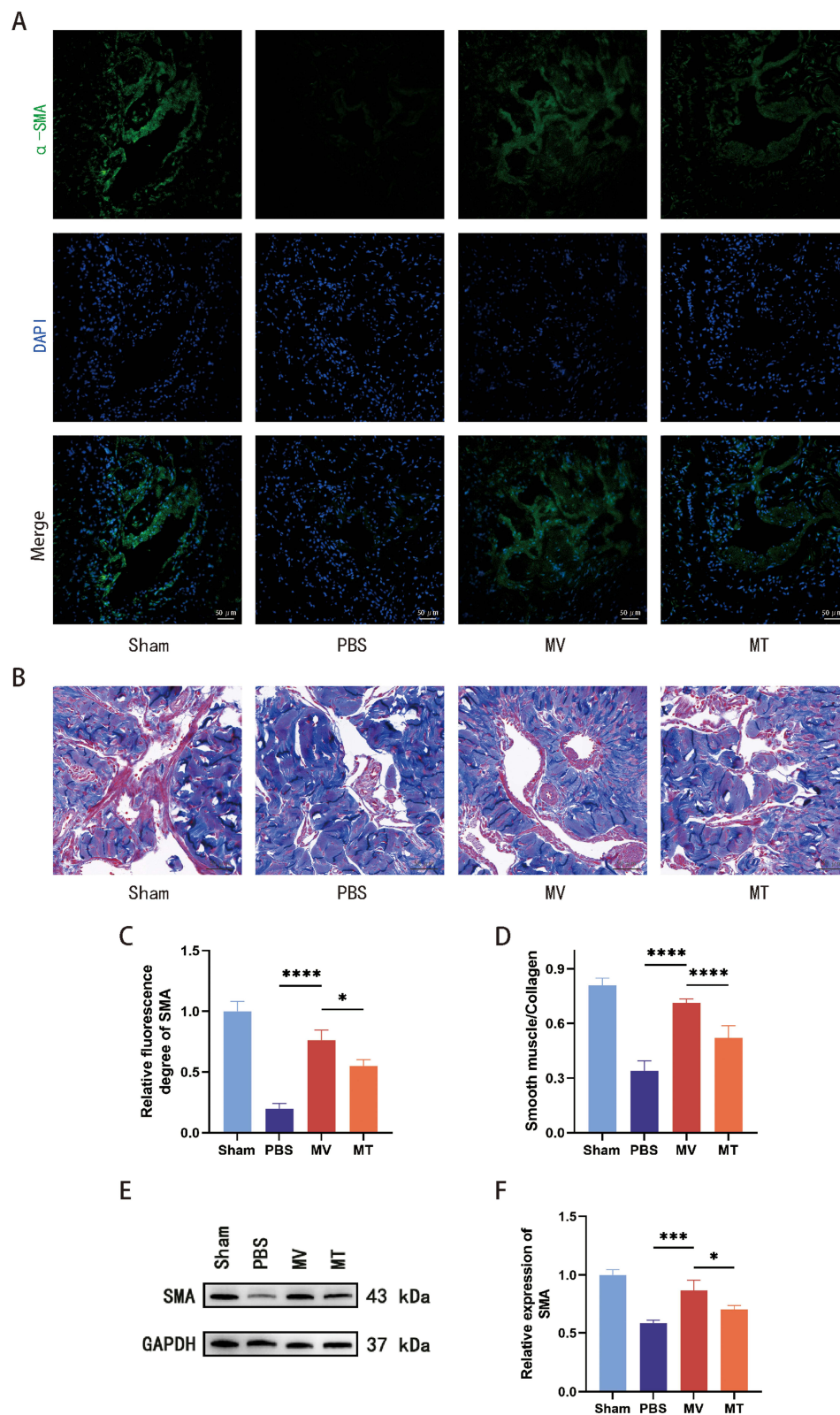
Figure 6 (**A** and **C**) Immunofluorescent staining and relative fluorescence degree of SMA of corpus cavernosum in the sham, PBS, MV, and MT groups, scale bar, 50 μm (n=3). (**B** and **D**) Masson's trichrome staining of corpus cavernosum, and the smooth muscle/collagen ratios in each group, scale bar, 50 μm (n=6). (**E** and **F**) Representative images and relative expression levels of Western blotting for SMA in the corpus cavernosum in each group (n=3). PBS, group injected with PBS. MV, group injected with MVs. MT, group injected with MT. *P<0.05, ***P<0.001, ****P<0.0001.
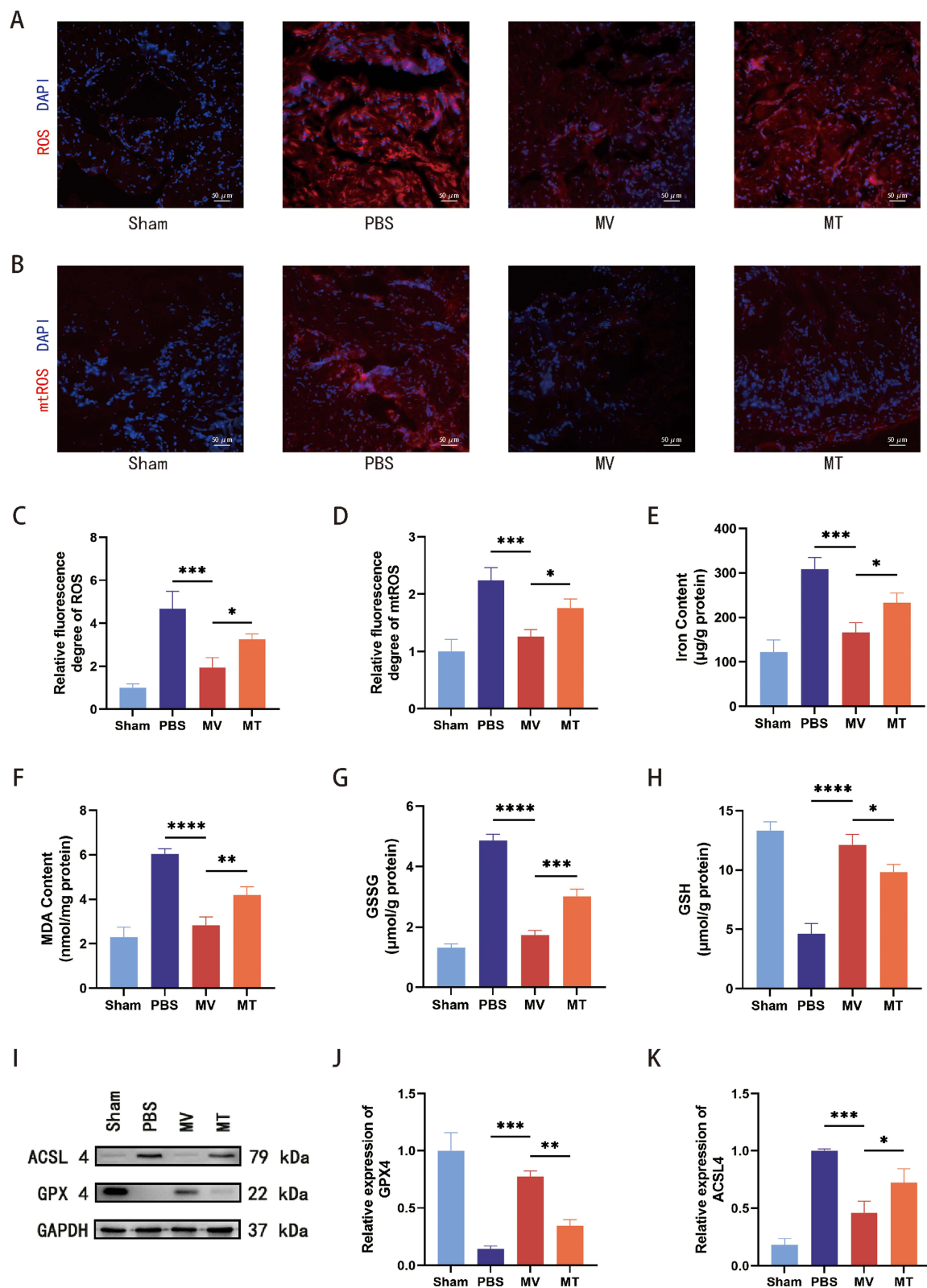
Figure 7 (**A** and **C**) Superoxide anion levels were detected using fluorescence analysis, scale bar, 100 μm (n=3). (**B** and **D**) Mitochondrial superoxide levels were detected using fluorescence analysis, scale bar, 100 μm (n=3). (**E-H**) The content of iron, MDA, GSSG, and GSH in corpus cavernosum of each group was measured (n=3). (**I-K**) Representative images of Western blot assays and relative protein expression levels of GPX4 and ACSL4 in corpus cavernosum of each group (n=3). PBS, group injected with PBS. MV, group injected with MVs. MT, group injected with MT. *P<0.05, **P<0.01, ***P<0.001, ****P<0.0001.
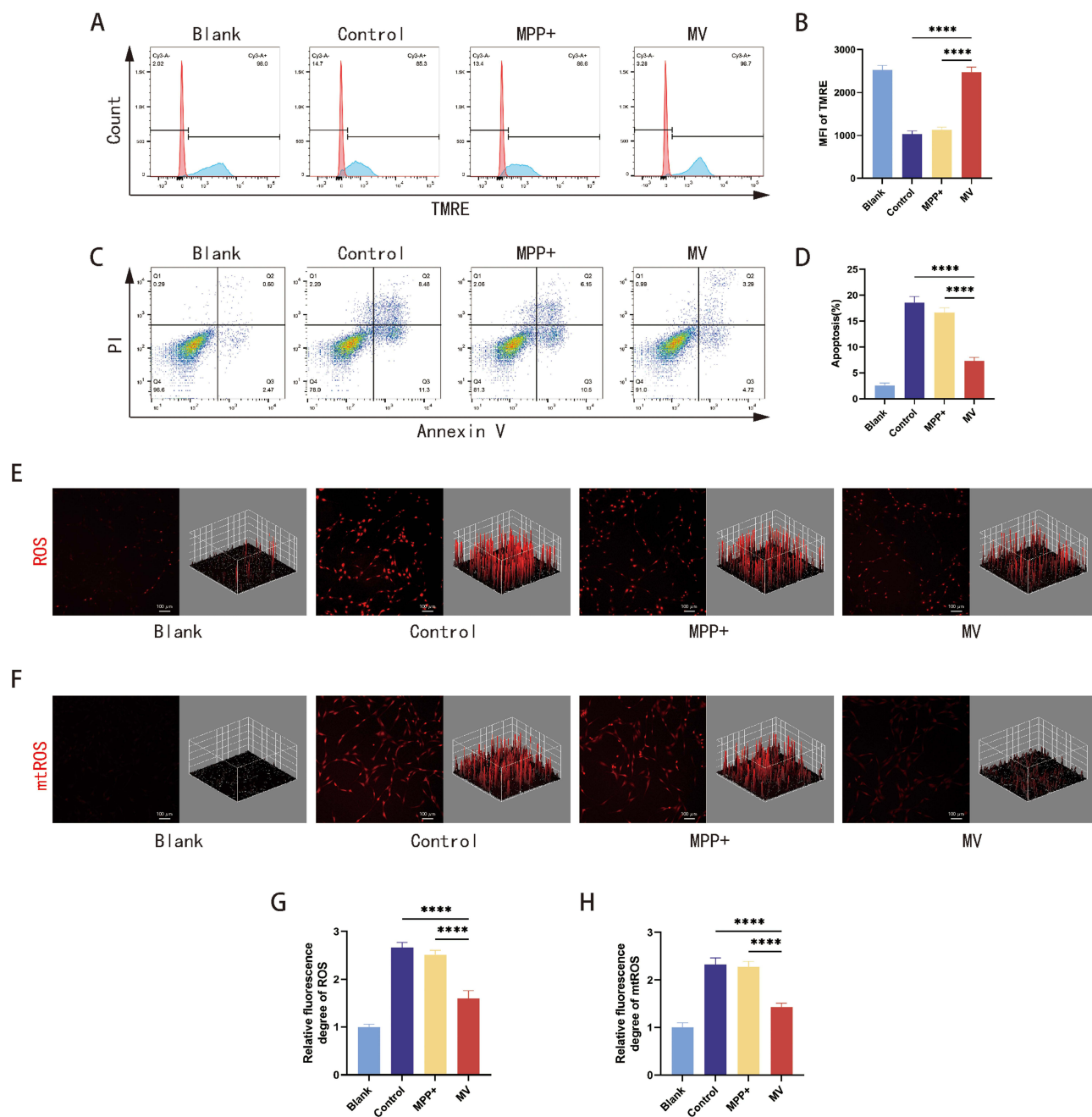
Figure 8 (**A** and **B**) The mitochondrial membrane potential of each group was analyzed (n=3). (**C** and **D**) Apoptosis in each group was analyzed (n=3). (**E** and **G**) Representative DHE staining and relative fluorescence degree in each group, scale bar, 100 μm (n=3). (**F** and **H**) Representative mitoSOX staining and relative fluorescence degree in each group, scale bar, 100 μm (n=3). Blank, CCSMCs without any treatment. Control, CCSMCs treated with H_2O_2 treatment. MPP+, CCSMCs pretreated with MPP+ MVs before treatment with H_2O_2 treatment.MV, CCSMCs pretreated with MVs before treating with H_2O_2 treatment. ****P<0.0001. MFI: mean fluorescence intensity.

CCSMCs with MPP+ MVs for 24 h, then treated CCSMCs with 0.5 μM RSL3 for 24 h, and detected the above related indicators. Iron, MDA, and GSSG contents increased in the MMP+ group, whereas GSH content decreased, which was contrary to the effect observed in the MV group (Figure 9A–D). In terms of cellular fluorescence, GPX4 fluorescence intensity was slightly enhanced in the MPP+ group, and ACSL4 fluorescence intensity was slightly decreased compared to the control group (Figure 9E–H). Although there was some effect, there was no statistically significant difference between the two groups (data not shown). Similarly, Western blotting showed that the expression of GPX4 decreased in the MPP+ group, whereas that of ACSL4 increased, almost reaching the level of the control group (Figure 9I–K). These results indicated that MVs' ability of MVs to enhance cellular resistance to OS and ferroptosis was significantly
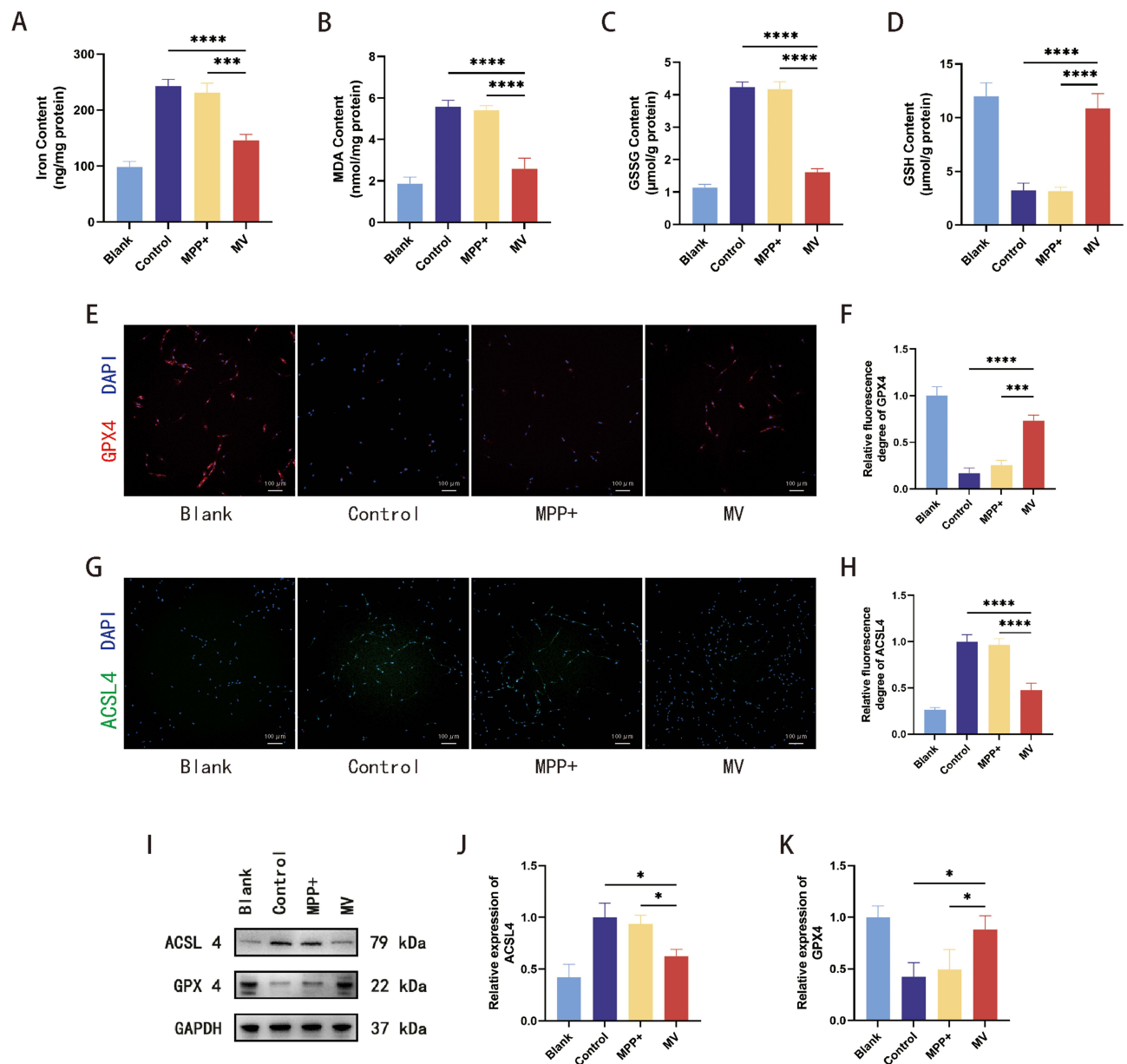
Figure 9 (**A-D**) The content of iron, MDA, GSSG, and GSH in CCSMCs was measured (n=3). (**E-H**) Representative fluorescence images and quantification of GPX4 and ACSL4 in CCSMCs of each group, scale bar, 100 μm (n=3). (**I-K**) Representative images of Western blot assays and relative protein expression levels of GPX4 and ACSL4 in CCSMCs of each group (n=3). Blank, CCSMCs without any treatment. Control, CCSMCs treated with RSL3. MPP+, CCSMCs pretreated with MPP+ MVs before treatment with RSL3. MV, CCSMCs pretreated with MVs before treatment with RSL3. *P<0.05, ***P<0.001, ****P<0.0001.

weakened after MPP+ inhibited its internal mitochondrial function, suggesting that MV transplantation works by transferring its internal mitochondria.

The same rescue experiments were performed on rats. We evaluated the ratio of ICP to MAP in rats 14 days after injection. The results in the MV group showed that ICPmax/MAP and total ICP/MAP were higher than those in the PBS group (Figure 10A–C). However, after pretreatment of MVs with MPP+, these ratios decreased significantly in the MPP+ group (Figure 10A–C). Immunofluorescence and Masson's trichrome staining results revealed that the expression of SMA and the ratio of smooth muscle to collagen were increased in the MV group compared to the PBS group, as mentioned above, whereas these results were significantly decreased in the MPP+ group compared to those in the MV group (Figure 10D–G). Similarly, Western blotting showed that the ability of MVs to restore the expression of SMA was significantly weakened after pretreatment with MPP+ (Figure 10H–I).
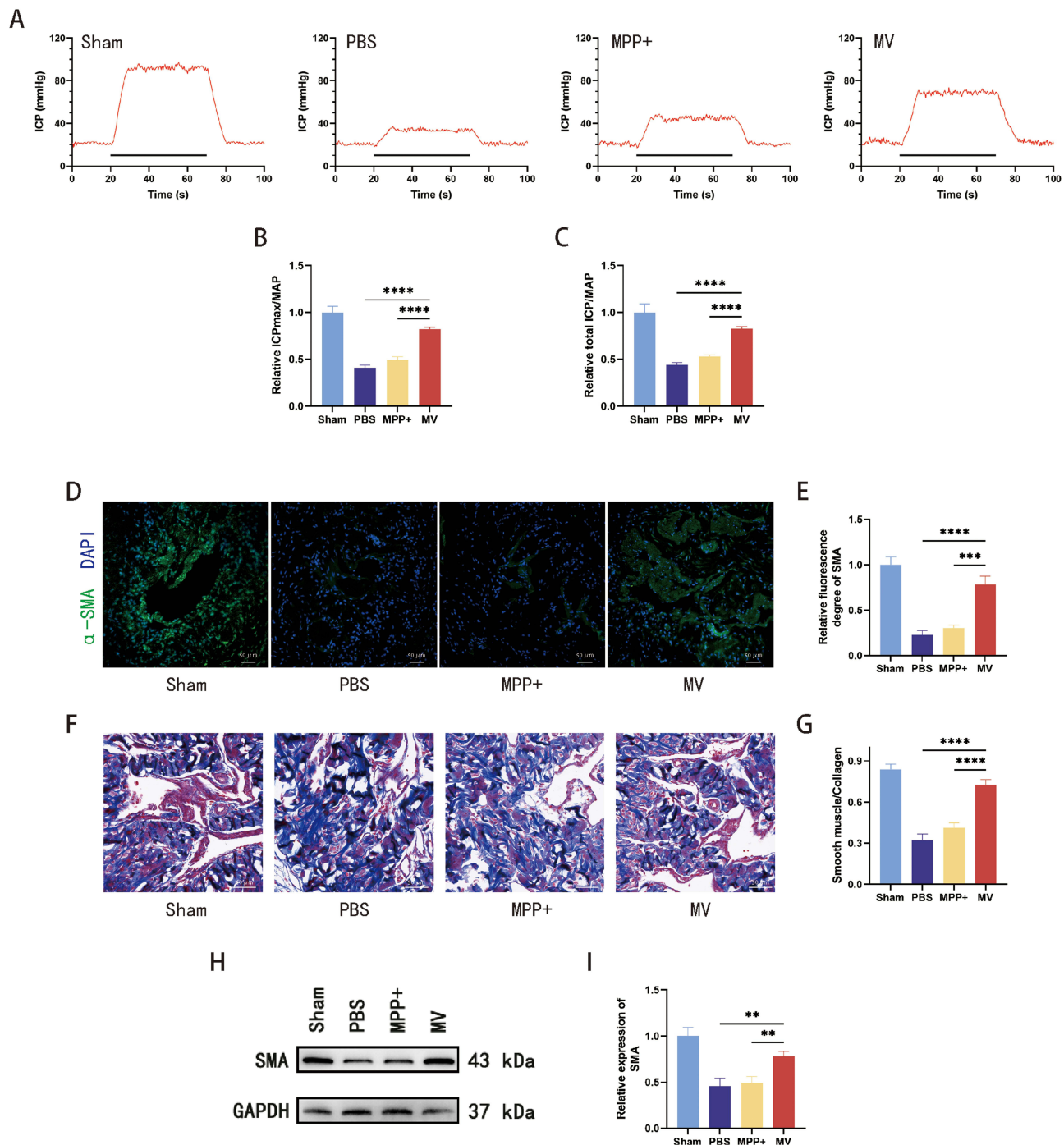
Figure 10 (**A**) ICP responses to electrostimulation in the Sham, PBS, MPP+, and MV groups. (**B** and **C**) Relative ICPmax to MAP ratio, and total ICP to MAP ratio responses to electrostimulation in four groups (n=6). (**D** and **E**) Representative fluorescence images and relative fluorescence degree of SMA of corpus cavernosum in the sham, PBS, MPP+, and MV groups, scale bar, 50 μm (n=3). (**F** and **G**) Masson's trichrome staining of corpus cavernosum, and the smooth muscle/collagen ratios in each group, scale bar, 50 μm (n=6). (**H** and **I**) Representative images and relative expression levels of Western blot analyses for SMA in the corpus cavernosum in each group (n=3). PBS, group injected with PBS. MPP+, group injected with MPP+ MVs. MV, group injected with MVs. **P<0.01, ***P<0.001, ****P<0.0001.

To study OS and ferroptosis in CC, we performed the corresponding experiments. Although ROS and mtROS in the CC were significantly downregulated in the MV group, ROS and mtROS in the CC in the MPP+ group were hardly reduced (Figure 11A–D). This showed that MPP+MV had little effect on reducing OS in CC. As mentioned above, compared with the PBS group, the MV group showed reduced iron, MDA, and GSSG content and increased GSH content in the CC (Figure 11E–H). However, the ability of MPP+ MVs to reverse these changes was significantly decreased to
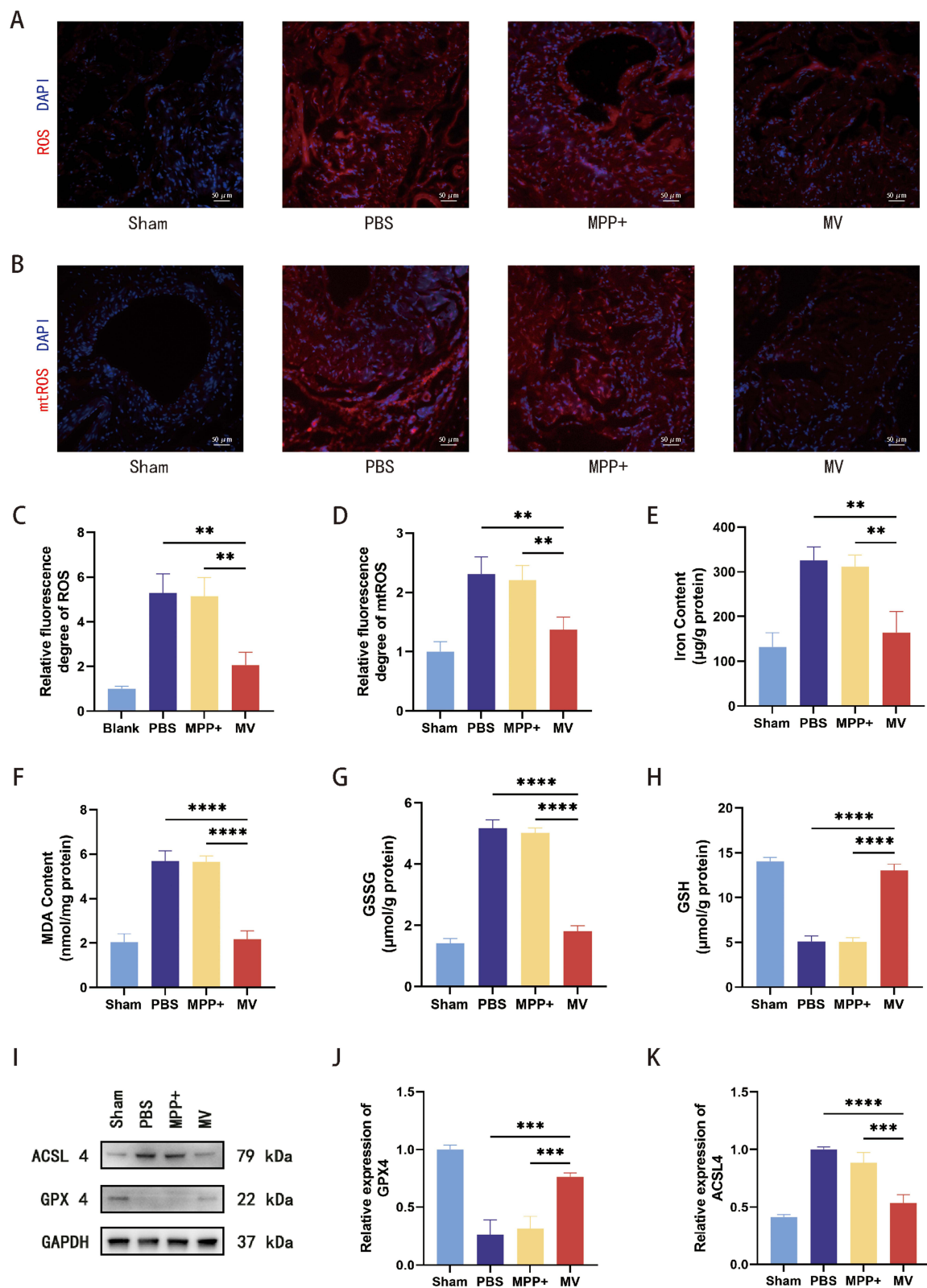
Figure 11 (**A** and **C**) Superoxide anion levels were detected using fluorescence analysis, scale bar, 100 μm (n=3). (**B** and **D**) Mitochondrial superoxide levels were detected using fluorescence analysis, scale bar, 100 μm (n=3). (**E-H**) The content of iron, MDA, GSSG, and GSH in corpus cavernosum of each group was measured (n=3). (**I-K**) Representative images of Western blot assays and relative protein expression levels of GPX4 and ACSL4 in the corpus cavernosum of each group (n=3). PBS, group injected with PBS. MPP+, group injected with MPP+ MVs. MV, group injected with MVs. **P<0.01, ***P<0.001, ****P<0.0001.
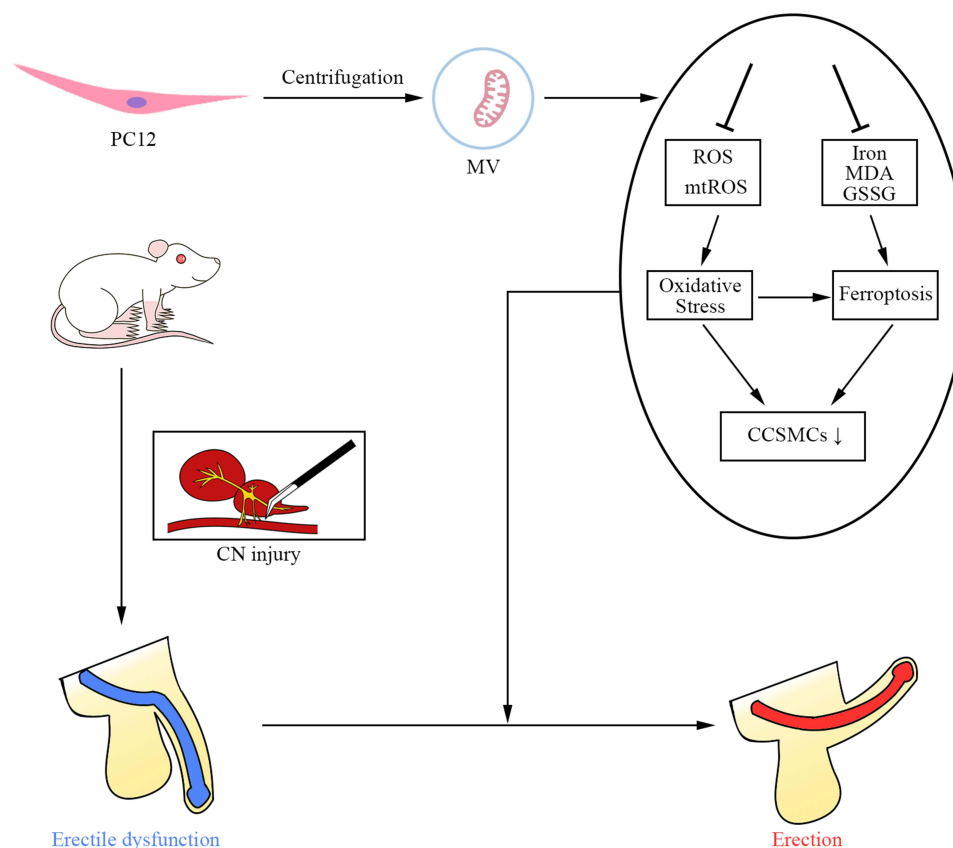
Figure 12 Schematic illustration of MVs for CNI ED treatment.

almost the same level as that in the PBS group (Figure 11E–H). Moreover, Western blotting showed that, compared to the MV group, the expression of the ferroptosis inhibitor GPX4 was significantly reduced in the MPP+ group, whereas that of the promoting factor ACSL4 was significantly elevated (Figure 11I–K). These results indicated that the ability of MVs to combat OS and ferroptosis after MPP+ pretreatment was significantly reduced in both in vivo and in vitro experiments, indicating that mitochondria may be the main way to exert the efficacy of MVs.

In conclusion, these results demonstrate for the first time that PC12-MVs can restore erectile function by delivering its contained mitochondria, reducing the OS levels of CCSMCs, reducing the occurrence of apoptosis and ferroptosis (Figure 12).

Discussion

CNI ED is a common complication affecting the physical and mental health of patients after pelvic surgery.[1,36] Although advanced surgical methods have been proposed to reduce the incidence of postoperative ED, damage to neurovascular bundles cannot be completely avoided.[4,5] However, current therapeutic methods for CNI ED have limited effects, and novel therapeutic schemes need to be explored.[2,6,7]

In our previous study, we found that CNI ED in rats could be treated by transplanting MT from adipose-derived stem cells (ADSCs), suggesting that MT transplantation therapy has some potential.[37] However, because the abundance of MT in ADSCs has not been determined, and CNI is accompanied by penile hypoxia, apoptosis, and OS, the survival rate of MT in the transplantation microenvironment is low, and the therapeutic effect is limited. Therefore, MV transplantation is a promising treatment option. Thomas et al reported that skeletal soft tissues absorbed EVs containing functional mitochondria using an acellular approach.[38] Furthermore, Ikeda et al reported that mitochondria-rich extracellular vesicles were better than isolated mitochondria in restoring the energy of ischemic myocardium.[16] Therefore, we suspected that MVs have a therapeutic advantage over MT alone. First, vesicle-like structures can better protect the

contents from irritation and damage to the microenvironment. Second, the presence of membrane-like structures was more efficient in transferring content. Finally, the MVs are easily transported and stored, thereby embodying the characteristics of ideal healthcare materials.[39,40] In this study, by comparing PC12-derived MVs and MT, we found that both MVs and MT could be internalized into CCSMCs to play a role, but the effect of MVs was superior to that of MT.

CCSMCs play an important role in penile erection, and SMA is a relatively rich component of CCSMCs. Therefore, whether SMA content is sufficient is a significant factor affecting erectile function.[33] Some studies have shown that CCSMCs within penile tissues are reduced after CNI.[41] Consistent with prior research, our CNI ED rat model revealed a significant decrease in SMA content in the PBS group compared with that in the sham group. Following the injection of MVs and MT, the SMA content increased to varying degrees. Notably, the SMA expression was higher in the MV group than in the MT group.

Studies have shown that OS is the key mechanism of CNI ED pathogenesis.[25] After CNI, the level of OS in the cavernosum is significantly increased, and a large number of oxygen free radicals are produced, thus reducing the CCSMCs involved in the erection process, resulting in the occurrence of CNI ED. OS can induce a variety of cell death, including apoptosis and ferroptosis.[42] It has been established that apoptosis in cavernosum is elevated in diabetic mice. The administration of drugs designed to inhibit apoptosis has been found to only partially inhibit cell death, with the resultant improvement in ED being insignificant.[43] This indicates that there are other death modes besides apoptosis in CCSMCs. Notably, ferroptosis has also been documented in diabetes-induced ED and CNI ED.[28–30] However, the role of MVs in ferroptosis in CNI ED remains unclear. In this study, we initially observed that MVs reduced iron content and levels of OS, both in vivo and in vitro, including ROS, mtROS, MDA, GSSG, and GSH. Subsequently, we found that the expression of GPX4 was upregulated and that of ACSL4 was downregulated by MVs both in vivo and in vitro. These results suggest that MVs may play a role in the treatment of CNI ED by inhibiting ferroptosis in CCSMCs.

Some scholars have proposed that, in addition to mitochondria, MVs also contain mitochondrial DNA (mtDNA) or RNA (mtRNA), and these ingredients may also play a therapeutic role.[44,45] To demonstrate that MVs act primarily through mitochondria, we successfully inhibited mitochondrial function within MVs using MPP+, as described previously.[15] We found that MVs pretreated with MPP+ did not achieve the therapeutic effect of MVs either in vivo or in vitro. Although there was still some efficacy compared to the PBS or control group, the difference was not statistically significant. These results suggest that mitochondria-related contents in MVs may play a minor role and that the therapeutic effect is mainly through the delivery of the mitochondria.

This study has certain limitations. First, experimental results derived from rat models may not comprehensively reflect the therapeutic efficacy observed in human patients. Second, we administered only one injection in the rat models, and the number of treatments and single doses in humans still needs to be further explored in future clinical practice. Furthermore, the mechanism underlying the delivery of mitochondria contained within MVs to recipient cells remains unexplored, as it falls outside the scope of the present study. However, this will be a focal area of our future research endeavors.

Conclusion

In conclusion, to our knowledge, this is the first study to elucidate the therapeutic effects of PC12-MVs transplantation in CNI ED. We found that MVs transplantation can inhibit the increase of oxidative stress level in CCSMCs, thereby reducing apoptosis. Furthermore, modulation of the GPX4/ACSL4 axis was found to diminish ferroptosis. Above effects are mainly achieved by delivering mitochondria. These results provide novel potential treatments for CNI ED and novel insights into the mechanisms of MVs treatment for CNI ED.

Institutional Review Board Statement

The animal study protocol was approved by the Ethics Committee of Experimental Animals at South China Agricultural University (2024D018).

Data Sharing Statement

Data supporting the findings of this study are available from the corresponding author upon request.

Author Contributions

All authors made a significant contribution to the work reported, whether that is in the conception, study design, execution, acquisition of data, analysis and interpretation, or in all these areas; took part in drafting, revising or critically reviewing the article; gave final approval of the version to be published; have agreed on the journal to which the article has been submitted; and agree to be accountable for all aspects of the work.

Disclosure

The authors declare no conflict of interest.

References

1. NIH Consensus Conference. Impotence. NIH consensus development panel on impotence. *JAMA*. 1993;270(1):83–90. doi:10.1001/jama.1993.03510010089036
2. Madiraju SK, Hakky TS, Perito PE, Wallen JJ. Placement of inflatable penile implants in patients with prior radical pelvic surgery: a literature review. *Sex Med Rev.* 2019;7(1):189–197. doi:10.1016/j.sxmr.2018.10.002
3. Zippe C, Nandipati K, Agarwal A, Raina R. Sexual dysfunction after pelvic surgery. *Int J Impot Res*. 2006;18(1):1–18. doi:10.1038/sj.ijir.3901353
4. Fang J, Wei B, Zheng Z, et al.; Chinese Postoperative Urogenital Function (PUF) Research Collaboration Group. Preservation versus resection of denonvilliers' fascia in total mesorectal excision for male rectal cancer: follow-up analysis of the randomized PUF-01 trial. *Nat Commun*. 2023;14(1):6667. doi:10.1038/s41467-023-42367-3
5. Wei B, Zheng Z, Fang J, et al.; Chinese Postoperative Urogenital Function (PUF) Research Collaboration Group. Effect of denonvilliers' fascia preservation versus resection during laparoscopic total mesorectal excision on postoperative urogenital function of male rectal cancer patients: initial results of Chinese PUF-01 randomized clinical trial. *Ann Surg*. 2021;274(6):e473–e480. doi:10.1097/SLA.0000000000004591
6. Lima TFN, Bitran J, Frech FS, Ramasamy R. Prevalence of post-prostatectomy erectile dysfunction and a review of the recommended therapeutic modalities. *Int J Impot Res*. 2021;33(4):401–409. doi:10.1038/s41443-020-00374-8
7. Raina R, Agarwal A, Zaramo CEB, Ausmundson S, Mansour D, Zippe CD. Long-term efficacy and compliance of MUSE for erectile dysfunction following radical prostatectomy: SHIM (IIEF-5) analysis. *Int J Impot Res*. 2005;17(1):86–90. doi:10.1038/sj.ijir.3901284
8. Gupta D, Zickler AM, El Andaloussi S. Dosing extracellular vesicles. *Adv Drug Deliv Rev*. 2021;178:113961. doi:10.1016/j.addr.2021.113961
9. Zhang X, Zhang H, Gu J, et al. Engineered extracellular vesicles for cancer therapy. *Adv Mater*. 2021;33(14):e2005709. doi:10.1002/adma.202005709
10. Harrell CR, Jovicic N, Djonov V, Arsenijevic N, Volarevic V. Mesenchymal stem cell-derived exosomes and other extracellular vesicles as new remedies in the therapy of inflammatory diseases. *Cells*. 2019;8(12):1605. doi:10.3390/cells8121605
11. Wang F, Cerione RA, Antonyak MA. Isolation and characterization of extracellular vesicles produced by cell lines. *STAR Protoc*. 2021;2(1):100295. doi:10.1016/j.xpro.2021.100295
12. Xu R, Greening DW, Zhu H-J, Takahashi N, Simpson RJ. Extracellular vesicle isolation and characterization: toward clinical application. *J Clin Invest*. 2016;126(4):1152–1162. doi:10.1172/JCI81129
13. Phinney DG, Di Giuseppe M, Njah J, et al. Mesenchymal stem cells use extracellular vesicles to outsource mitophagy and shuttle microRNAs. *Nat Commun*. 2015;6(1):8472. doi:10.1038/ncomms9472
14. Kowal J, Arras G, Colombo M, et al. Proteomic comparison defines novel markers to characterize heterogeneous populations of extracellular vesicle subtypes. *Proc Natl Acad Sci*. 2016;113(8):E968–977. doi:10.1073/pnas.1521230113
15. O'Brien CG, Ozen MO, Ikeda G, et al. Mitochondria-rich extracellular vesicles rescue patient-specific cardiomyocytes from doxorubicin injury: insights into the SENECA trial. *JACC CardioOncol*. 2021;3(3):428–440. doi:10.1016/j.jaccao.2021.05.006
16. Ikeda G, Santoso MR, Tada Y, et al. Mitochondria-rich extracellular vesicles from autologous stem cell-derived cardiomyocytes restore energetics of ischemic myocardium. *J Am Coll Cardiol*. 2021;77(8):1073–1088. doi:10.1016/j.jacc.2020.12.060
17. Wiatrak B, Kubis-Kubiak A, Piwowar A, Barg E. PC12 cell line: cell types, coating of culture vessels, differentiation and other culture conditions. *Cells*. 2020;9(4):958. doi:10.3390/cells9040958
18. Cheng X-T, Huang N, Sheng Z-H. Programming axonal mitochondrial maintenance and bioenergetics in neurodegeneration and regeneration. *Neuron*. 2022;110(12):1899–1923. doi:10.1016/j.neuron.2022.03.015
19. Xian X, Cai -L-L, Li Y, et al. Neuron secrete exosomes containing miR-9-5p to promote polarization of M1 microglia in depression. *J Nanobiotechnol*. 2022;20(1):122. doi:10.1186/s12951-022-01332-w
20. Gollihue JL, Patel SP, Eldahan KC, et al. Effects of mitochondrial transplantation on bioenergetics, cellular incorporation, and functional recovery after spinal cord injury. *J Neurotrauma*. 2018;35(15):1800–1818. doi:10.1089/neu.2017.5605

21. Campbell JD, Burnett AL. Neuroprotective and nerve regenerative approaches for treatment of erectile dysfunction after cavernous nerve injury. *Int J Mol Sci*. 2017;18(8):1794. doi:10.3390/ijms18081794

22. Valko M, Leibfritz D, Moncol J, Cronin MTD, Mazur M, Telser J. Free radicals and antioxidants in normal physiological functions and human disease. *Int J Biochem Cell Biol*. 2007;39(1):44–84. doi:10.1016/j.biocel.2006.07.001

23. Forman HJ, Zhang H. Targeting oxidative stress in disease: promise and limitations of antioxidant therapy. *Nat Rev Drug Discov*. 2021;20 (9):689–709. doi:10.1038/s41573-021-00233-1

24. Liu S, Li K, Zhao Y, et al. Fermented gynochthodes officinalis (F.C.How) Razafim. & B.Bremer Alleviates diabetic erectile dysfunction by attenuating oxidative stress and regulating PI3K/Akt/eNOS pathway. *J Ethnopharmacol*. 2023;307:116249. doi:10.1016/j.jep.2023.116249

25. Wang Y, Meng X-H, Zhang Q-J, et al. Losartan improves erectile function through suppression of corporal apoptosis and oxidative stress in rats with cavernous nerve injury. *Asian J Androl*. 2019;21(5):452–459. doi:10.4103/aja.aja_8_19

26. Stockwell BR, Jiang X, Gu W. Emerging mechanisms and disease relevance of ferroptosis. *Trends Cell Biol*. 2020;30(6):478–490. doi:10.1016/j.tcb.2020.02.009

27. Ashraf A, Jeandriens J, Parkes HG, So P-W. Iron dyshomeostasis, lipid peroxidation and perturbed expression of cystine/glutamate antiporter in alzheimer's disease: evidence of ferroptosis. *Redox Biol*. 2020;32:101494. doi:10.1016/j.redox.2020.101494

28. Feng H, Liu Q, Deng Z, et al. Human umbilical cord mesenchymal stem cells ameliorate erectile dysfunction in rats with diabetes mellitus through the attenuation of ferroptosis. *Stem Cell Res Ther*. 2022;13(1):450. doi:10.1186/s13287-022-03147-w

29. Xu W, Sun T, Wang J, et al. GPX4 alleviates diabetes mellitus-induced erectile dysfunction by inhibiting ferroptosis. *Antioxidants*. 2022;11 (10):1896. doi:10.3390/antiox11101896

30. Chen P, Chen Z, Zhai J, Yang W, Wei H. Overexpression of PRDX2 in adipose-derived mesenchymal stem cells enhances the therapeutic effect in a neurogenic erectile dysfunction rat model by inhibiting ferroptosis. *Oxid Med Cell Longev*. 2023;2023:4952857. doi:10.1155/2023/4952857

31. Chen Z, Zhai J, Ma J, et al. Melatonin-primed mesenchymal stem cells-derived small extracellular vesicles alleviated neurogenic erectile dysfunction by reversing phenotypic modulation. *Adv Healthcare Mater*. 2023;12(12). doi:10.1002/adhm.202203087

32. Muralidharan-Chari V, Clancy J, Plou C, et al. ARF6-regulated shedding of tumor cell-derived plasma membrane microvesicles. *Curr Biol*. 2009;19 (22):1875–1885. doi:10.1016/j.cub.2009.09.059

33. C Flaccid, Erectile Dysfunction. *Nat Rev Dis Primers*. 2016;2(1):16004. doi:10.1038/nrdp.2016.4

34. Musicki B, Bhunia AK, Karakus S, Burnett AL. S-nitrosylation of NOS pathway mediators in the penis contributes to cavernous nerve injury-induced erectile dysfunction. *Int J Impot Res*. 2018;30(3):108–116. doi:10.1038/s41443-018-0021-y

35. Liu X, Gao X, Pang J, et al. Proteomic analysis of rat penile tissue in a model of erectile dysfunction after radical prostatectomy. *BJU Int*. 2007;99 (6):1500–1505. doi:10.1111/j.1464-410X.2007.06775.x

36. Nam RK, Cheung P, Herschorn S, et al. Incidence of complications other than urinary incontinence or erectile dysfunction after radical prostatectomy or radiotherapy for prostate cancer: a population-based cohort study. *Lancet Oncol*. 2014;15(2):223–231. doi:10.1016/S1470-2045(13)70606-5

37. Zhai J, Chen Z, Chen P, Yang W, Wei H. Adipose derived mesenchymal stem cells-derived mitochondria transplantation ameliorated erectile dysfunction induced by cavernous nerve injury. *World J Mens Health*. 2024;42(1):188–201. doi:10.5534/wjmh.220233

38. Thomas MA, Fahey MJ, Pugliese BR, Irwin RM, Antonyak MA, Delco ML. Human mesenchymal stromal cells release functional mitochondria in extracellular vesicles. *Front Bioeng Biotechnol*. 2022;10:870193. doi:10.3389/fbioe.2022.870193

39. Crewe C, Funcke J-B, Li S, et al. Extracellular vesicle-based interorgan transport of mitochondria from energetically stressed adipocytes. *Cell Metab*. 2021;33(9):1853–1868.e11. doi:10.1016/j.cmet.2021.08.002

40. D'Souza A, Burch A, Dave KM, et al. Microvesicles transfer mitochondria and increase mitochondrial function in brain endothelial cells. *J Control Release*. 2021;338:505–526. doi:10.1016/j.jconrel.2021.08.038

41. Ferrini MG, Kovanecz I, Sanchez S, Umeh C, Rajfer J, Gonzalez-Cadavid NF. Fibrosis and loss of smooth muscle in the corpora cavernosa precede corporal veno-occlusive dysfunction (CVOD) induced by experimental cavernosal nerve damage in the rat. *J Sex Med*. 2009;6(2):415–428. doi:10.1111/j.1743-6109.2008.01105.x

42. Liu K, Cui K, Feng H, et al. JTE-013 supplementation improves erectile dysfunction in rats with streptozotocin-induced type I diabetes through the inhibition of the rho-kinase pathway, fibrosis, and apoptosis. *Andrology*. 2020;8(2):497–508. doi:10.1111/andr.12716

43. Li H, Chen L-P, Wang T, Wang S-G, Liu J-H. Calpain inhibition improves erectile function in diabetic mice via upregulating endothelial nitric oxide synthase expression and reducing apoptosis. *Asian J Androl*. 2018;20(4):342–348. doi:10.4103/aja.aja_63_17

44. D'Acunzo P, Pérez-González R, Kim Y, et al. Mitovesicles are a novel population of extracellular vesicles of mitochondrial origin altered in down syndrome. *Sci Adv*. 2021;7(7):eabe5085. doi:10.1126/sciadv.abe5085

45. Jang SC, Crescitelli R, Cvjetkovic A, et al. Mitochondrial protein enriched extracellular vesicles discovered in human melanoma tissues can be detected in patient plasma. *J Extracell Vesicles*. 2019;8(1):1635420. doi:10.1080/20013078.2019.1635420